Nuclear Physics B98 (1975) 93–99

A MEASUREMENT OF THE PROTON-PROTON CROSS SECTION AT THE CERN ISR

K. EGGERT, H. FRENZEL, K.L. GIBONI and W. THOMÉ
III. Physikalisches Institut der Technischen Hochschule, Aachen, Germany

B. BETEV *, P. DARRIULAT, P. DITTMANN, M. HOLDER,
K.T. McDONALD and H.G. PUGH **
CERN, Geneva, Switzerland

T. MODIS and K. TITTEL
Institut für Hochenergie Physik, Heidelberg, Germany

V. ECKARDT, H.J. GEBAUER, R. MEINKE, O.R. SANDER ***
and P. SEYBOTH
Max-Planck-Institut für Physik und Astrophysik, Munich, Germany

Received 1 August 1975

We present a measurement of the total cross section σ_t in proton-proton collisions at the CERN ISR. The method involves determination of the total interaction rate and machine luminosity. A two-arm scintillation hodoscope observes ~ 90% of the total interaction rate, while a streamer chamber is employed for event topologies missed by the main trigger. An increase of about 10% in σ_t is observed in the energy range $\sqrt{s}$ = 23.6 to $\sqrt{s}$ = 62.8 GeV/c in agreement with previous experiments.

We present a measurement of the total proton-proton cross section at various ISR energies, using the Van der Meer method [1]. This method consists of moving the beam apart vertically, while recording the interaction rate as a function of relative beam displacement. This permits measurements of the machine luminosity L. We infer then the total cross section σ_t from an observation of the total interaction rate R via the relation $\sigma_t = R/L$.

Most interactions are identified by a coincidence between two large sets of scintillation counters on each downstream side of the intersection. Additional interactions which fail to give such a coincidence are studied with a streamer chamber de-

* On leave from Institute of Nuclear Research, Sofia, Bulgaria.
** On leave from University of Maryland, College Park, Md., USA.
*** Now at UCLA, Los Angeles, Calif., USA.

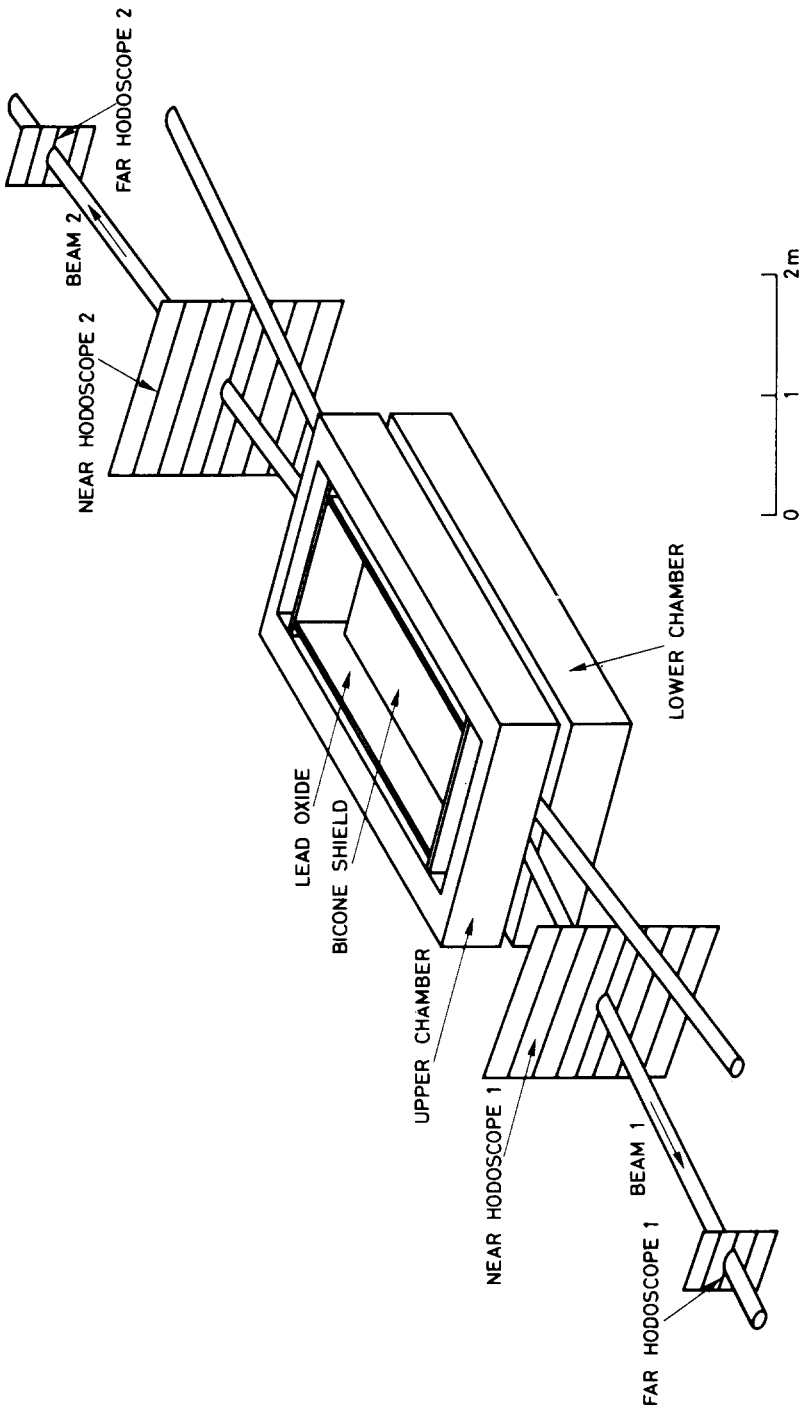

Fig. 1. Schematic layout of the apparatus.

tector which surrounds the intersection and is triggered with minimum bias. Rejection of background is achieved in the first case by strict timing requirements and in the second by the requirement that the observed tracks extrapolate to the region where the beams intersect (the "diamond"). Finally, the contribution due to small-angle events which escape both the scintillators and the streamer chambers, is computed from published elastic and inelastic data.

The experimental set-up is shown in fig. 1. There are two scintillation counter hodoscopes on each downstream side of the intersection region. The "near" hodoscopes at 3.0 m from the intersect are 150 cm wide and 140 cm high and consist of eight horizontal counters each, with phototubes on each end to improve time resolution. The "far" hodoscopes at 5.4 m from the intersect are 50 cm wide and 60 cm high and consist of four horizontal counters each. All counters are made up of two layers to suppress accidentals from induced radioactivity. The beam pipes go through the hodoscopes and fit tightly to an elliptical hole (7 cm × 16 cm). The "near" and "far" hodoscopes together cover production angles between 6 and 250 mrad.

The two double-gap streamer chambers [2], above and below the beam plane, almost cover the full solid angle. Each chamber is 50 cm high, 270 cm long (along the beams) and 125 cm wide. The dependence of the acceptance upon production angle is governed by the 8 cm gap between the chambers. Over most of the angular range it is 86%, but it falls steeply in the forward direction vanishing below 40 mrad. Lead-oxide plates, one radiation length thick, convert γ rays (produced from π^0 decays) in the sensitive volumes of the chambers. Particles produced in a beam-beam interaction must traverse the lead-oxide plates or the thick elliptical beam pipe before reaching the scintillation hodoscopes. As a result, the hodoscopes have a substantial efficiency for detecting neutrals as well as charged particles.

Signals from the "far" and "near" hodoscopes on side 1 of the intersect are OR'ed after appropriate time equalization to produce an ARM 1 signal, and similarly for ARM 2. The time difference between the ARM 1 and ARM 2 signals has a characteristic distribution (fig. 2) with a three-peak structure. The central peak corresponds to equal timing and is mostly due to genuine beam-beam interactions producing particles detected in the two arms. The side peaks, displaced by 18 nsec, result from stray particles travelling outside the beam pipes and traversing both near hodoscopes in sequence. Evidence for this interpretation is provided when the beams are steered away from each other; this causes the central peak to disappear, while the side peaks remain approximately constant (fig. 2b). The probability that stray particles also traverse one or both of the "far" hodoscopes is negligible, so that multiple side peaks are not observed. A time window of ±10 nsec around the central peak was used to select beam-beam interactions and to reject background due to the stray particles.

For most runs beam conditions were so good that the side peaks were hardly visible (fig. 2a) and the central peak exhibits a FWHM of 7 nsec. We have checked that in such conditions the ±10 nsec window contains the central peak to better

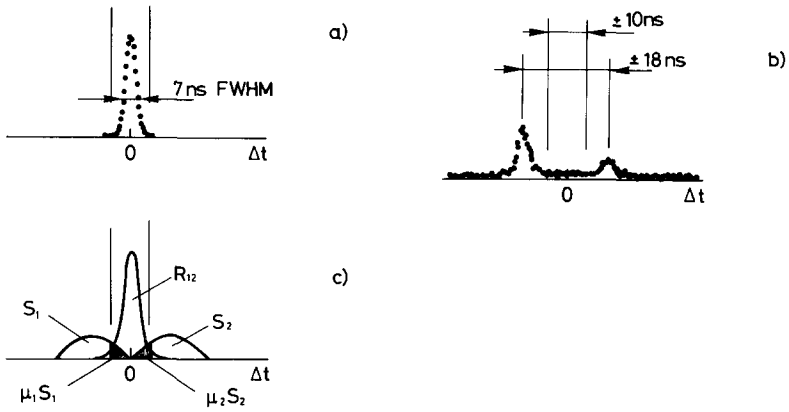

Fig. 2. ARM 1 – ARM 2 time-of-flight distributions: (a) with colliding beams (the side peaks are too low to be visible); (b) with beams at maximum displacement (no beam-beam interactions); (c) schematic time-of-flight distribution showing the contribution of the side peaks to the measured coincidence rate.

than 2‰. The rate of accidental coincidences between the arms was obtained by measuring the coincidence rate R'_{12} between an ARM 1 signal not coincident with an (ARM 1 · ARM 2) signal and a delayed ARM 2 signal not coincident with an (ARM 1 · ARM 2) signal either. As the measurements are usually performed in excellent beam conditions and with low beam currents (3 to 5 A) accidental rates do not exceed 1‰. In fact, most of the ARM single rates are due to beam-beam interactions.

When the beams are displaced vertically in the Van der Meer measurement, the rate R_{12} of ARM 1 · ARM 2 coincidence decreases and it becomes increasingly important to ensure that nothing other than genuine beam-beam interactions contribute to it. To study this effect we have measured R_{12} for well-centred beams before and after dumping one of the beams. The rate for a single beam was about 1‰ of the value before dumping the second beam. Streamer chamber pictures of the events associated with these residual triggers showed that they mostly correspond to stray particles accompanying the beam and producing high multiplicity interactions in the material near the intersect (vacuum chamber walls, lead-oxide plates, etc.), with produced particles passing outwards from the intersect through the hodoscopes and simulating real events. The contribution from beam-gas collisions is negligible under normal vacuum conditions (7×10^{-12} Torr). We conclude from the above that the contribution to R_{12} from interactions other than genuine beam-beam events should be proportional to the flux of stray particles accompanying each beam and therefore to the rates S_1 and S_2 in the side peaks,

$$R_{12} - R'_{12} = R_{12}\,(\text{beam-beam}) + \mu_1 S_1 + \mu_2 S_2 \,, \qquad (1)$$

where μ_1 and μ_2 are constants independent of beam displacement and R_{12} (beam-beam) is the true beam-beam rate.

The background terms in eq. (1) were normally extremely small when the beams were centred, but at large vertical displacements they sometimes become an appreciable fraction of R_{12}, causing difficulty in determining the area under the curve of R_{12} (beam-beam) versus relative beam displacement, which is needed in the Van der Meer measurement. The shape of the curve was therefore determined using auxiliary telescopes which saw a smaller fraction of the total cross section than the ARM, but had directional sensitivity to select particles produced in the "diamond" so that they counted only genuine beam-beam interactions. We then have

$$R_{12}(\text{beam-beam}) = \lambda T\,, \tag{2}$$

where T is the coincidence rate between the auxiliary telescopes and λ is a constant depending only on the beam energies. By combining eqs. (1) and (2) we obtain

$$R_{12} - R'_{12} = \lambda T + \mu_1 S_1 + \mu_2 S_2\,,$$

which should be satisfied by a single set of parameters λ, μ_1, and μ_2, at a given energy, independent of beam displacement. Fits show this to be true with reasonable χ^2.

The measurements were performed several times at each beam energy, usually shortly after scraping the beam edges so that T dropped sharply to zero when the beams were displaced. The area under the curves were determined by numerical integration to an accuracy of better than 0.5%. We applied the Van der Meer method on the displacement curves of T to obtain the cross section observed by telescope T. We then used the values of λ determined from the fit described above to calculate the cross sections as seen by the whole hodoscope. The reproducibility between different measurements at the same beam energy is always better than 1.5%.

In addition to those events detected in R_{12}, beam-beam interactions may produce an ARM signal on one side only or even no ARM signal at all. In each category they may or may not produce particles visible in the streamer chamber detector. We have measured the rate of those which do and rely on calculation for those which do not.

Interactions with a single ARM signal are observed by triggering the streamer chambers on an (ARM 1 · $\overline{\text{ARM 2}}$) coincidence. The photographs are scanned, measured, and processed with facilities and software described in previous publications [2, 3]. We select those pictures which have at least two tracks meeting inside the "diamond". From the resulting sample we subtract a contamination of (ARM 1 · ARM 2) type interactions occurring in the 2 μsec interval between the trigger and the appearance of the HV pulse in the streamer chambers. Protection against beam-beam interactions occurring before the trigger is obtained by application of a 10 μsec dead time, longer than the chamber memory time. We estimate that 10% of the single ARM rate produces less than two visible tracks in the streamer chamber detector and is therefore lost. This loss reflects the slightly smaller acceptance

Table 1
Total cross section as a function of c.m. energy

	Observed cross section		Corrections				
$\sqrt{s}$ (GeV)	(ARM 1 · ARM 2) (mb)	Single ARM (mb)	No ARM (mb)	σ_{obs} (mb)	Elastic losses (mb)	Inelastic losses (mb)	σ_t (mb)
23.6	33.9 ± 0.5	3.2 ± 0.4	0.3 ± 0.2	37.3 ± 0.6	0.9 ± 0.1	0.6 ± 0.3	38.7 ± 0.7
30.8	35.6 ± 0.5	1.7 ± 0.2	0.3 ± 0.2	37.6 ± 0.6	1.8 ± 0.1	0.6 ± 0.2	40.0 ± 0.6
45.2	36.4 ± 0.7	1.5 ± 0.2	0.3 ± 0.2	38.2 ± 0.7	3.3 ± 0.2	1.1 ± 0.3	42.5 ± 0.8
53.2	36.4 ± 0.6	1.0 ± 0.1	0.3 ± 0.2	37.6 ± 0.6	3.9 ± 0.2	1.4 ± 0.3	42.9 ± 0.7
62.8	36.4 ± 0.7	1.0 ± 0.2	0.3 ± 0.2	37.6 ± 0.7	4.7 ± 0.3	1.8 ± 0.4	44.1 ± 0.9

Various contributions to the observed cross sections, as well as calculated corrections for elastic and inelastic losses, are listed independently.

of the streamer chamber compared to that of the counter hodoscope. The estimate of the loss is based on a study made on samples of streamer chamber pictures obtained with beam-beam triggers where the events without visible tracks due to elastic and singly diffractive events were already accounted for.

Interactions with no ARM signal at all are studied with a similar method. The streamer chambers are triggered at random with a pulse generator vetoed by the (ARM 1 · ARM 2) coincidence. A single measurement is performed at 15.4 GeV beam energy. Out of 2700 triggers, 53 show at least two tracks meeting inside the "diamond" and have one or both hodoscopes hit. This is consistent with the expected contamination from single ARM type interactions occurring during the chamber memory time and against which no protection is provided, and from (ARM 1 · ARM 2) interactions occurring in the time interval between trigger and HV pulse. Eight events are observed with tracks only at large angles which miss both hodoscopes. From this we estimate a corresponding cross section of 0.25 ± 0.19 mb and assume this result to be valid at all energies.

Interactions with no ARM trigger or visible tracks in the streamer chambers are mostly due to elastic scattering where the scattered protons stay inside the beam pipes. Their rate is calculated from published values of the elastic cross section [4] by taking into consideration the detailed geometry of the detector. Inelastic losses of the single diffraction type of events, where no particle is observable in the streamer chamber, are estimated from published data [5]. The errors quoted in table 1 reflect predominantly uncertainties in the values of the diffraction cross section used. These losses increase with energy.

We have investigated possible sources of errors in addition to those previously mentioned. Uncertainties in the values of the beam currents, the clock calibration, space charge effects, and dependence upon the absolute vertical position of the beams, were all found to be negligible. A correction of the order of $\frac{1}{4}$ mb with an un-

certainty of comparable size was applied to account for the hysteresis in the ISR magnets defining the beam positions. This estimate was made by comparing runs where the displacement points were followed in different sequences. Finally, we have observed that when the beams are displaced simultaneously in all intersects the measured luminosity is lower by $(32 \pm 5)\%/E$ (GeV), as compared to the case where the beams are displaced in our intersect only. The correction has been applied when necessary.

The results of the measurements are summarized in table 1. The total cross section rises from 38.7 ± 0.7 mb at $\sqrt{s} = 23.6$ GeV to 44.1 ± 0.9 mb at $\sqrt{s} = 62.8$ GeV, in agreement with previously reported results [6].

We thank G. Vesztergombi and J. Kaltwasser for contributing to the running of the experiment, K. Potter and Ph. Bryan for information concerning the performance of luminosity measurements, the ISR staff for providing smooth running conditions, and the scanning teams of CERN and Aachen for scanning and measuring the streamer chamber pictures.

Partial financial support was given by the Bundesministerium fur Forschung und Technologie.

References

[1] S. van der Meer, CERN-ISR-PO/68-31 (June 1968) unpublished.

[2] K. Eggert, W. Thomé, B. Betev, G. Bohm, P. Darriulat, P. Dittmann, E. Gygi, M. Holder, K. T. McDonald, T. Modis, H.G. Pugh, F. Schneider, H. Albrecht, K. Tittel, I. Derado, V. Eckardt, H.J. Gebauer, R. Meinke, O.R. Sander and P. Seyboth, Nucl. Instr. 126 (1975) 477.

[3] K. Eggert, H. Frenzel, W. Thomé, B. Betev, P. Darriulat, P. Dittmann, M. Holder, K.T. McDonald, T. Modis, H.G. Pugh, K. Tittel, I. Derado, V. Eckardt, H.J. Gebauer, R. Meinke, O.R. Sander and P. Seyboth, Nucl. Phys. B86 (1975) 201.

[4] U. Amaldi, R. Biancastelli, C. Bosio, G. Matthiae, J.V. Allaby, W. Bartel, G. Cocconi, A.N. Diddens, R.W. Dobinson and A.M. Wetherell, Phys. Letters 44B (1973) 112;
G. Barbiellini, M. Bozzo, P. Darriulat, G. Diambrini-Palazzi, G. de Zorzi, A. Fainberg, M.I. Ferrero, M. Holder, A. McFarland, G. Maderni, S. Orito, J. Pilcher, C. Rubbia, A. Santroni, G. Sette, A. Staude, P. Strolin and K. Tittel, Phys. Letters 39B (1972) 663.

[5] M.G. Albrow, Invited talk presented at 5th Int. Symp. on many-particle hadrodynamics, Eisenach, Leipzig, 1974, and references therein.

[6] U. Amaldi, R. Biancastelli, C. Bosio, G. Matthiae, J.V. Allaby, W. Bartel, G. Cocconi, A.N. Diddens, R.W. Dobinson and A.M. Wetherell, Phys. Letters 44B (1973) 112;
S.R. Amendolia, G. Bellettini, P.L. Braccini, C. Bradaschia, R. Castaldi, V. Cavasinni, C. Cerri, T. Del Prete, L. Foa, P. Giromini, P. Laurelli, A. Menzione, G. Finocchiaro, P. Grannis, D. Green, R. Mustard and R. Thun, Phys. Letters 44B (1973) 119; Nuovo Cimento 17A (1973) 735.